



## Determinants and impact of Fog, Mist and Haze phenomena : The case of Rajiv Gandhi International Airport, Hyderabad

KAVITHA CHANDU, DHARMA RAJU A. \*, S. V. J. KUMAR\*\*,

G. CH. SATYANARAYANA\*\*\* and MADHAVAPRASAD DASARI

*GITAM Institute of Science, GITAM (deemed to be) University, Vishakhapatnam – 530 045, Andhra Pradesh, India*

*\*India Meteorological Department, Ministry of Earth Sciences, Hyderabad – 501 218, Telangana, India*

*\*\*India Meteorological Department, Ministry of Earth Sciences, Vishakhapatnam – 530 017, Andhra Pradesh, India*

*\*\*\*Center for Atmospheric Science, K L Deemed to be University, Guntur, India*

*(Received 2 September 2021, Accepted 28 September 2022)*

**e mail : [kchandu@gitam.edu](mailto:kchandu@gitam.edu)**

**सार** – अध्ययन का उद्देश्य राजीव गांधी अंतर्राष्ट्रीय हवाई अड्डे, हैदराबाद पर नौ वर्षों में तीन घटनाओं - कोहरे, धुंध और धुंध और हवाई यातायात पर उनके प्रभाव का विश्लेषण करना है। खराब दृश्यता की लंबी अवधि की घटनाओं का हवाई अड्डे की दिनचर्या से सतही इन-सीटू डेटा का उपयोग करके विश्लेषण किया जाता है। मौसम संबंधी अवलोकन, उपग्रह इमेजरी, पिछड़े प्रक्षेपवक्र, पुनर्विश्लेषित डेटा और वायु संबंधी आरेख। जलवायु संबंधी आंकड़ों ने मुख्य रूप से लंबे समय तक चलने वाले कोहरे की घटनाओं की व्याख्या की। वायुमंडल की स्थिर परतें, ग्रहों की सीमा परत में नमी की उपलब्धता, हल्की हवाएं, विचलन (नीचे की ओर गति/अवतलन) और विकिरण संबंधी शीतलन ने कोहरे के गठन और इसके निर्वाह का समर्थन किया। कम दृश्यता ने अध्ययन स्थल पर उड़ान में देरी और परिणामी आर्थिक नुकसान के कारण हवाई यातायात को बाधित किया।

**ABSTRACT.** The study aims to analyze the three phenomena - fog, mist and haze over nine years and their impact on air traffic at Rajiv Gandhi International Airport, Hyderabad. Longer duration events of deteriorated visibility are analysed using surface in-situ data from the airport routine meteorological observations, satellite imageries, backward trajectories, reanalysed data and aerological diagrams. The climatological data predominantly explained long-lasting fog events. The stable layers of the atmosphere, availability of moisture in the planetary boundary layer, light winds, divergence (downward motion/subsidence) and radiational cooling supported the formation of fog and its sustenance. Low visibility disrupted air traffic at the study site by way of flight delays and consequential economic loss.

**Key words** – Fog, Mist, Haze, Rajiv Gandhi International Airport, Backward trajectory.

### 1. Introduction

The clearance of aircraft to fly depends on visibility, especially during late night and early morning hours. Poor visibility causes flight delays, diversions, cancellations, rescheduling and ultimately monetary loss. Air traffic disruptions are frequently reported there during the winter season worldwide in general and in India in particular. Winter increases poor visibility events over most parts of India, including a land-locked state like Telangana, where radiational cooling occurs.

Fog, mist and haze are crucial determinants of horizontal visibility impacting aviation, although heavy rains and thunderstorms exacerbate adverse weather conditions. Scattering and absorption of light by particles such as water droplets, dust and soot reduces visibility. Scattering is the dominant effect of fog, while absorption plays a significant role in haze formation. Fog formation is mainly due to condensation and haze is entirely different and requires no condensation. Most of the time, haze occurs in areas, away from sources of air pollutants. The main difference between mist and fog is that mist

contains more moisture, has less density and dissipates more quickly than fog. In urban and industrial areas, smoke can provide plenty of nuclei, which helps form fog and mist.

Several studies have focussed on the three phenomena regarding their meteorological aspects, forecasting models, diagnostic facets and prognosis using satellites and NWP models. Tyagi *et al.*, 2017 attempted to analyze the role of black carbon and PM<sub>2.5</sub> particulates in the deterioration of visibility over the NCR, Delhi. The influence of prevailing synoptic conditions and boundary-layer characteristics on the spatiotemporal distribution of persistently longer duration fog events over Jiangsu province of China were analyzed (Peng *et al.*, 2016). Availing the HYSPLIT model, (Wang and Chen, 2014) have analyzed the fog events over the Jinan province of China (Shukla and Agnihotri, 2021). Characterized fog over Bengaluru city using the upper air sounding data. (Ram and Mohapatra, 2008) Analyzed the characterization of fog over Guwahati airport. Kulkarni *et al.*, 2019 reported the loss of aviation economy at New Delhi airport due to fog during the 2011-2016 winters. The meteorological parameters favoring fog formation over Kempegowda International airport, Bengaluru, India, were studied and analyzed (Kutty *et al.*, 2019). However, investigations centering on examining their impact on airports in flight departure delays are scant.

In light of the above, the present study aims at the (i) frequency of occurrence of the three phenomena, (ii) conditions that favored their duration for a longer time and (iii) their combined impact of air traffic disruptions (Flight delays) during the winter season for the period 2011-19 at Rajiv Gandhi International Airport (RGIA), Hyderabad.

## 2. Location and data methodology

The flight operations started at Rajiv Gandhi International airport (RGIA) (17° 14' 5.9" N, 78° 25' 17.9" E) located at Shamshabad, about 30 km south of Hyderabad, Telangana, India, from the present location in 2008. Previously, national and international flights were operated from Begumpet. Today, it is the sixth busiest airport in India. Hyderabad is geographically located in southern Telangana on the Deccan Plateau with an average elevation of 540 meters. The Shamshabad airport is within the Greater Hyderabad Municipal Corporation (GHMC) limits en route to Mahabubnagar district.

The study will be carried out for winter months over nine years from 2011-2019. The frequency of occurrence, time of onset, duration of event, visibility and dew point

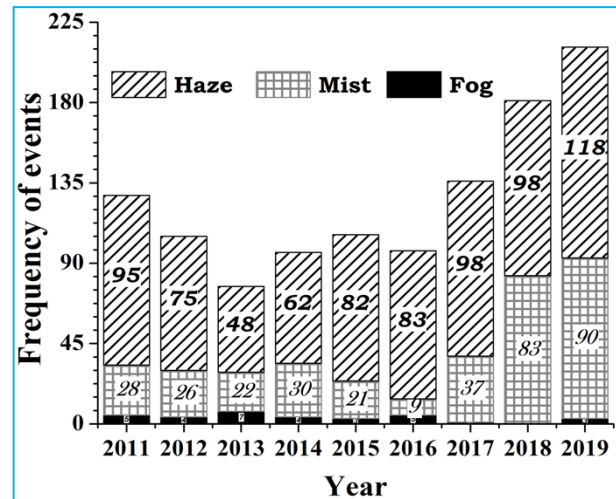


Fig. 1. The yearly frequencies of Fog, Mist and Haze events during 2011-2019

temperature, air temperature, wind speed and direction data collected from the current weather register of the meteorological office, India Meteorological Department, RGIA. The Hybrid Single-Particle Lagrangian Integrated Trajectory (HYSPLIT) are drawn, availing the online software tool of the Air Resources Laboratory (ARL) of the National Oceanic and Atmospheric Administration (NOAA), USA ([http://ready.arl.noaa.gov/HYSPLIT\\_traj.php](http://ready.arl.noaa.gov/HYSPLIT_traj.php)). Upper air data for calculating Fog Stability Index (FSI) is collected from the web link (<http://weather.uwyo.edu/upperair/sounding.html>). The INSAT-3D satellite images of low clouds/fog are obtained from the website (<http://www.mosdac.gov.in>). The fifth generation of the ECMWF global climate reanalysis (ERA5) is utilized (<https://www.ecmwf.int/en/forecasts/datasets/reanalysis-datasets/era5>) to study the thermo-dynamical features of fog.

## 3. Results and discussion

### 3.1. Frequency of occurrence of fog, mist and haze events

#### 3.1.1. Events by year

During the 2011-2019 winter months, fog events fluctuated between zero in 2018 and 7 in 2013. The haze events, which starting with a frequency of 95 in 2011, declined to 48 in 2013. The events shot up to 62 in the next year and continuously recorded an increasing trend during the period. Mist events fluctuated between 9 in 2016 and 90 in 2019. The total number of events reported by fog was 32, while mist and haze events were 346 and 759 respectively (Fig. 1). Thus, fog is less frequent than the other two phenomena during the period of study.

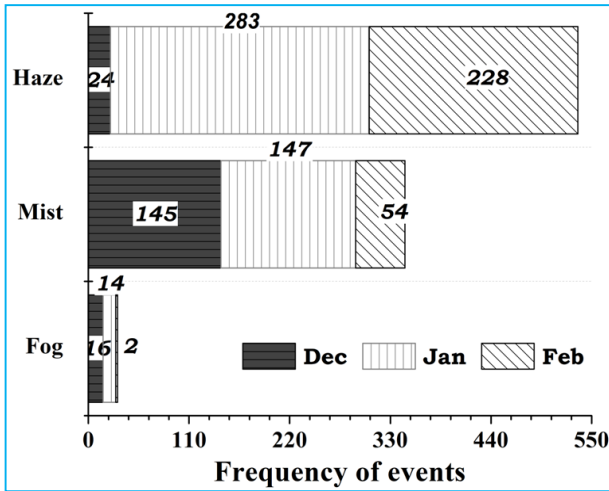


Fig. 2. The monthly frequencies of Fog, Mist and Haze events during 2011-2019

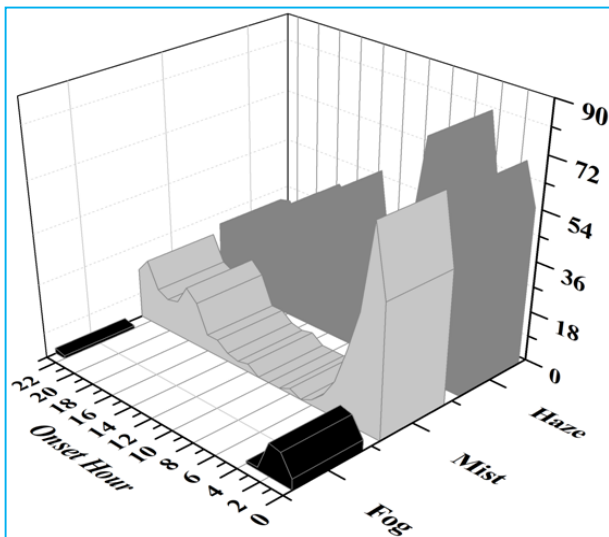


Fig. 3. The hourly frequencies of the onset of Fog, Mist and Haze events during 2011-2019

### 3.1.2. Events by month

During the winter season of the reference period, the monthly occurrence of three phenomena varied. It is evident from Fig. 2 that fog formation is more frequent in December, followed closely by January of the year. On the other hand, mist and haze occurrences peaked in January.

### 3.1.3. Events by hour

During the study period, the onset of fog (Fig. 3) is between 2200 and 0400 UTC, perhaps manifesting the role of radiational cooling. However, the most preferred

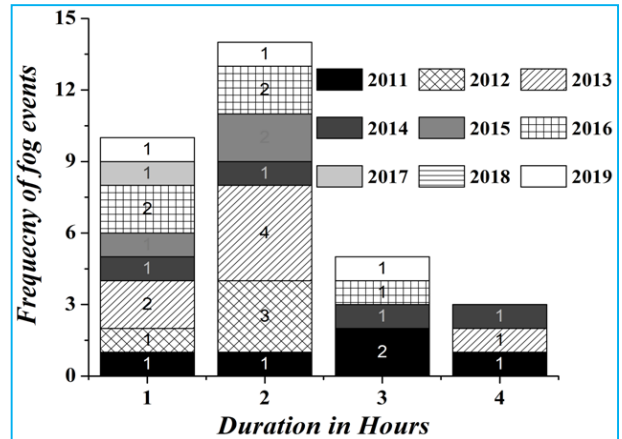


Fig. 4. Duration of fog event by Annual

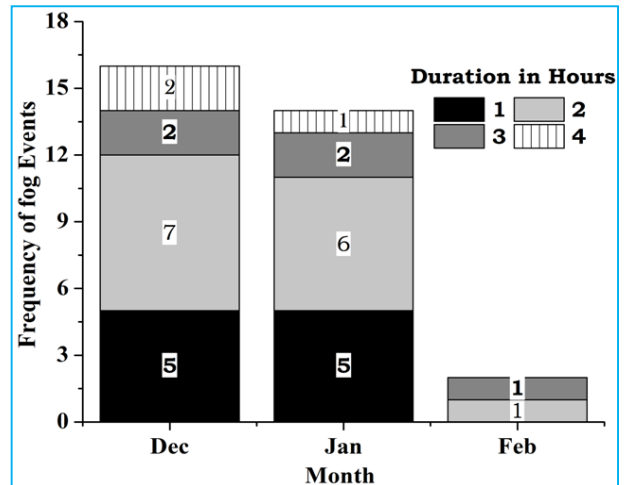


Fig. 5. Duration of fog event by month

time for fog formation is between 0000 and 0200 UTC, as 84.3% of fog events were reported during these hours. Turning to mist, 46.5% of cases were between 0000 and 0200 UTC and the rest concentrated after sunset. The onset of haze was at all hours of a day. Out of 759 haze events, 46.2% were reported between 0000 and 0500 UTC (before sunrise).

### 3.1.4. Duration of events

Fig. 4 shows the duration of fog by year. As observed earlier, fog occurred during December and January months except in 2018. The events had a duration ranging from one hour to four hours. Days with episodes lasting one and two hours are the most common and the least frequent are episodes lasting four hours. Three episodes of a four-hour-long fog events were recorded in 2011, 2013 and 2014. The pattern is similar by month also (Fig. 5). Fig. 6 shows the number of events with mist

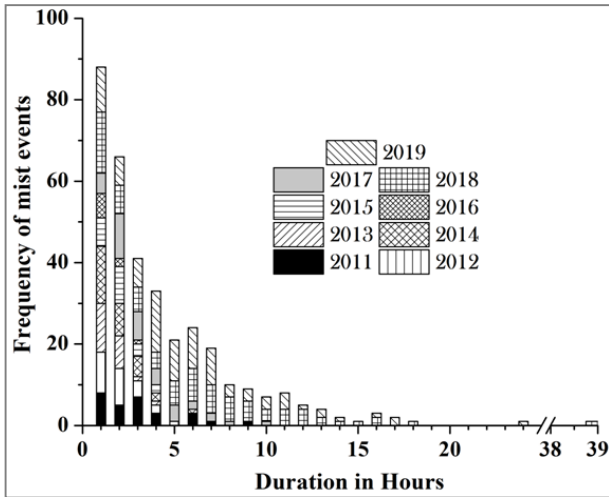


Fig. 6. Duration of mist event by year

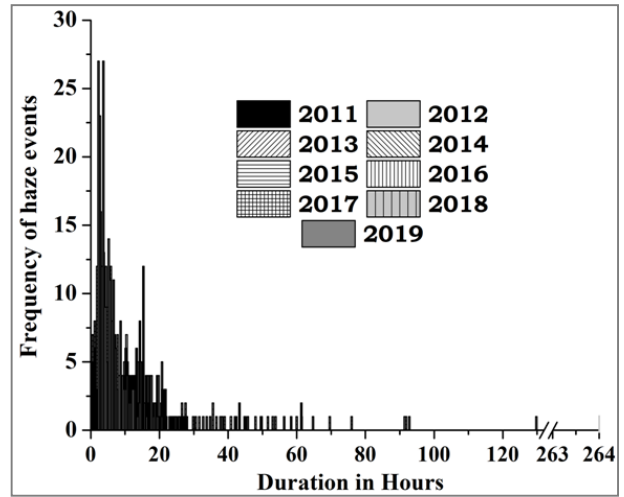


Fig. 8. Duration of Haze event by annual

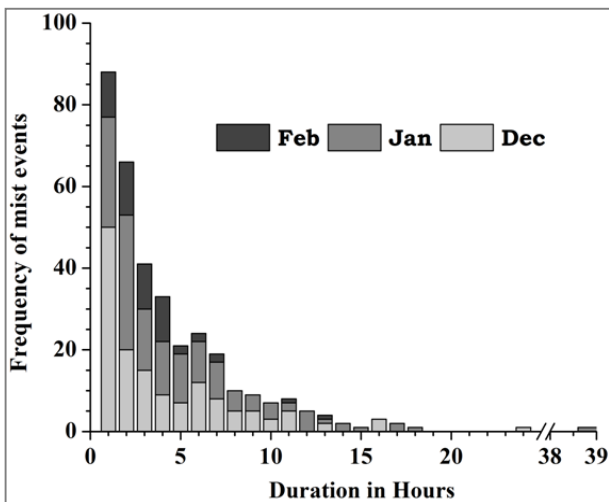


Fig. 7. Duration of mist event by month

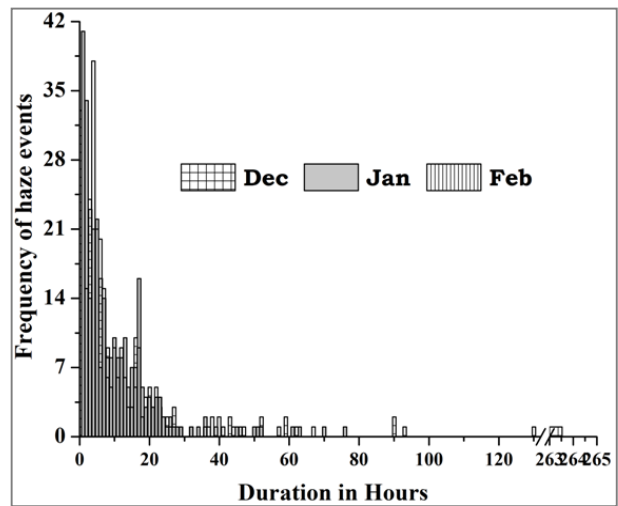


Fig. 9. Duration of Haze event by month

episodes by year and duration. Mist occurred every month (Fig. 7) of the year in the winter season at the study site. The events had a duration ranging from a minimum of an hour to a maximum of 39 hours. However, mist events lasting one and two hours were the most common and the least frequent are episodes lasting fourteen or more hours. The longest (39 h), persistent and a widespread mist event was recorded in January 2018.

A rare haze event lasted for 264 hours during the winter season of 2012 (Fig. 8). Haze events ranged from one hour to 264 hrs, with events between one and two hours being the most common and least frequent are episodes lasting 23 or more hours. Haze occurred during

every month (Fig. 9) of the winter season from 2011 to 2019.

### 3.2. Long duration mist and haze events : Role of climatology

The role of climatological data, such as wind speed, wind direction and dew point temperature during the long and persistent mist and haze events in 2018 and 2012, respectively, have been carried out to understand the conditions that favored their occurrence.

In the presence of mist, the wind speed was less than 10 m/s very slow (< 5m/s) and relatively light winds

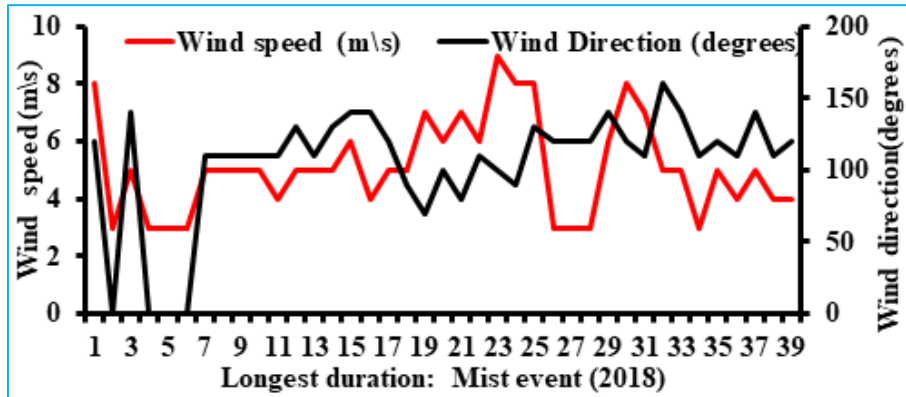


Fig. 10. Magnitude and direction of the wind during the 39-hour mist event

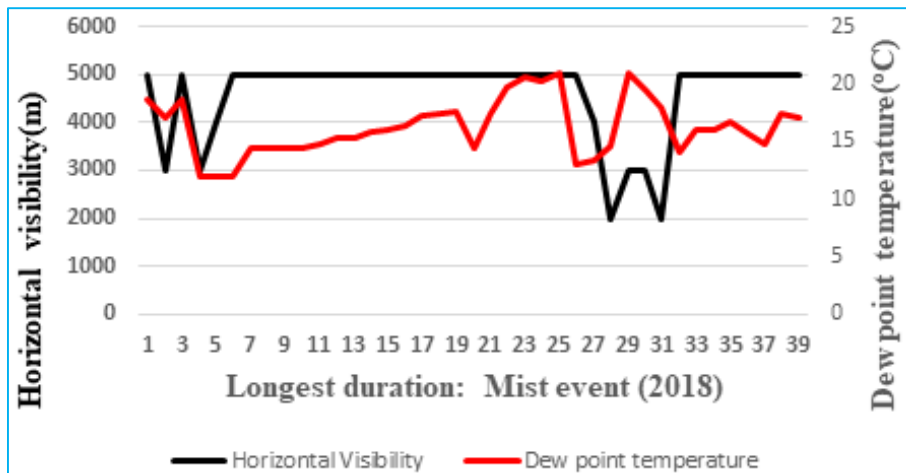


Fig. 11. Horizontal visibility and dew point temperature during the 39-hour mist event

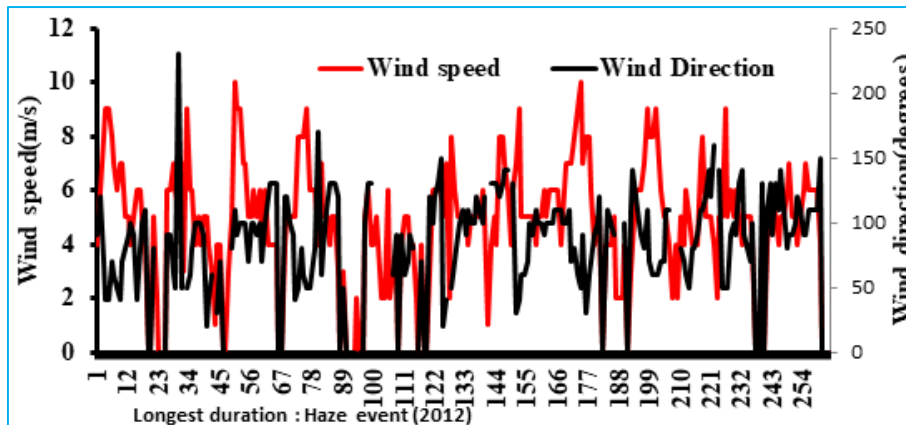


Fig. 12. Magnitude and direction of the wind during a 264-hour lasting haze event

(<10 m/s) prevailed during the event. The frequency of occurrence of very light wind is 69.7%. Fig. 10 shows that the wind direction is east-south-easterly during the entire

event. Dew point temperature (Fig. 11) represents the amount of moisture in the air. The higher the dew point, the higher is the moisture content in the air. The

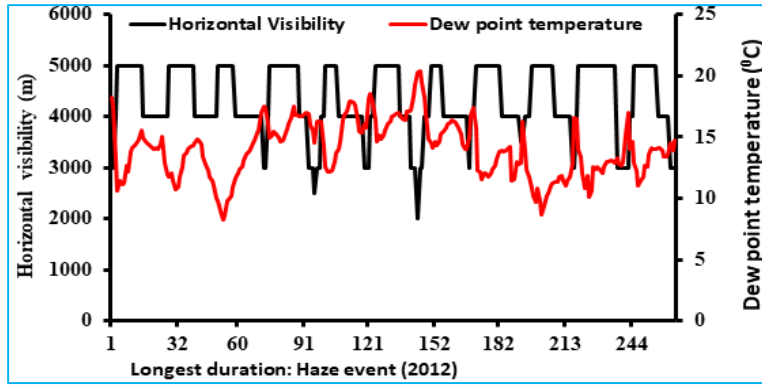
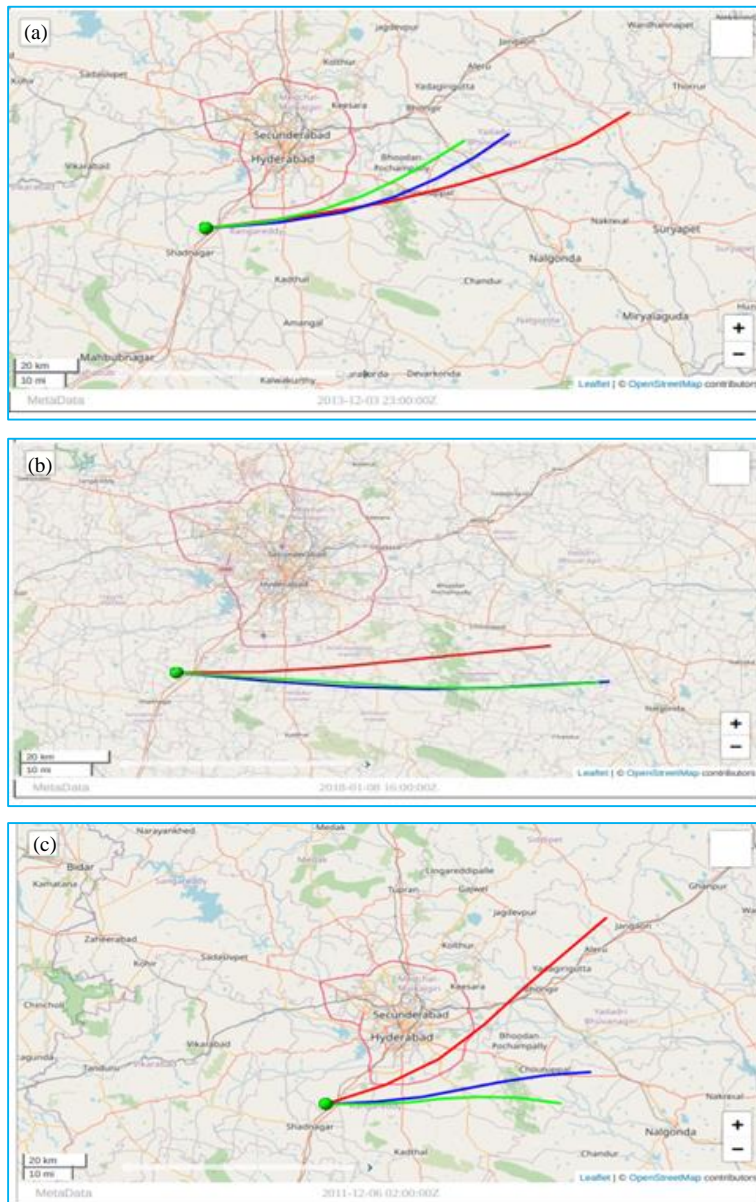
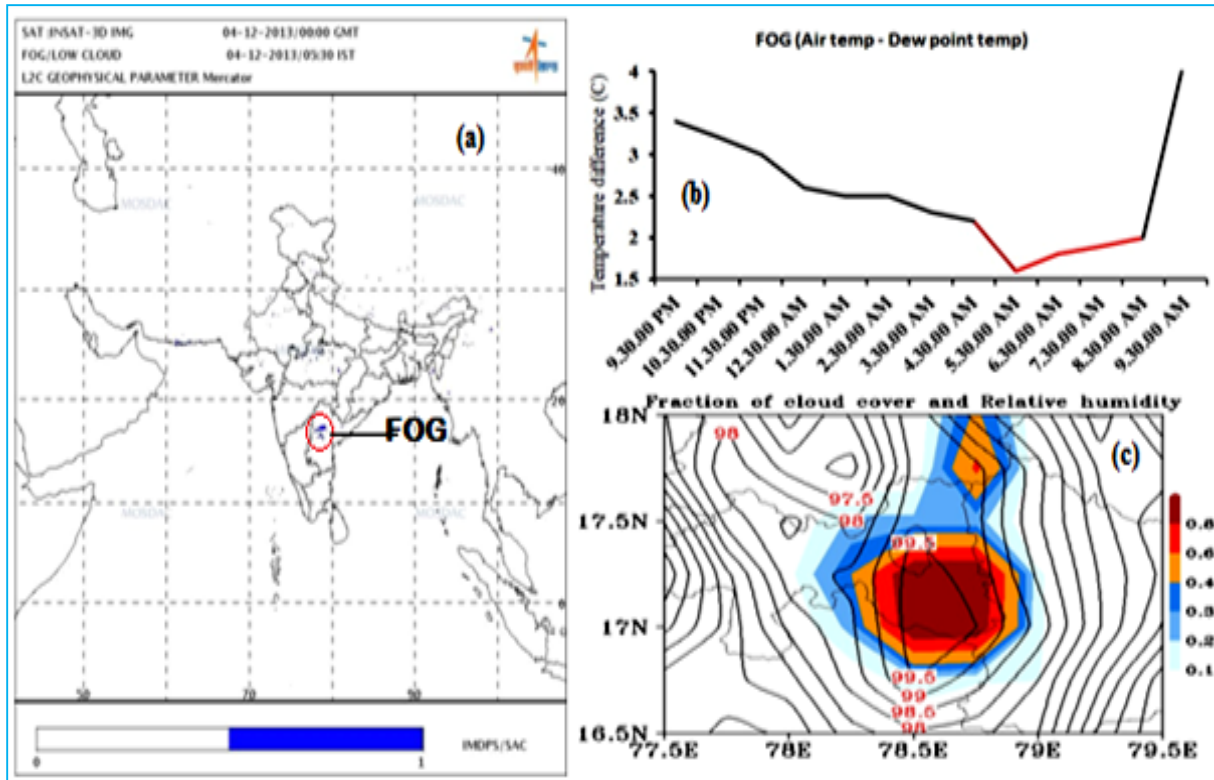


Fig. 13. Horizontal visibility and dew point temperature during a 264-hour lasting Haze event



Figs. 14(a-c). The HYSPLIT backward trajectories of long-duration (a) Fog, (b) Mist and (c) Haze events



**Figs. 15(a-c).** Fog identification through observation of (a) INSAT-3D Satellite imagery (b) Meteorological parameters (METARS) and (c) Fraction of cloud cover and relative humidity (operational product of ERA5)

dew point temperature ranged from 20.9 °C to 12 °C. The horizontal visibility during mist varied from 5000 m to 2000 m. Visibility varied directly with dew point temperature with a time lag, clearly showing the impact of moisture content on mist formation.

The wind speed was less than 10 m/s, very light (< 5m/s) and relatively light winds (<10 m/s) prevailed during the long haze event. The frequency of occurrence of calm wind is 64.7%. Fig. 12 shows that the predominant wind direction is east-south-easterly during the event and the dew point temperature (Fig. 13) ranged from 20.4 °C to 8.2 °C. When the dew point temperature is low, horizontal visibility has increased and *vice versa*. Thus, other meteorological factors such as wind speed and wind direction (east- south-easterly winds) determined the haze formation and its magnitude apart from dew point temperature.

Further back trajectory analysis helps track the transport pathways during the long-duration events of the study. Figs. 14(a-c) shows the backward trajectories (HYSPLIT) plotted for an hour ahead of the long-duration fog [4<sup>th</sup> December, 2013, 0000 UTC (onset hour)], Mist [8<sup>th</sup> January, 2018, 1700 UTC (onset hour)] and Haze

**TABLE 1**

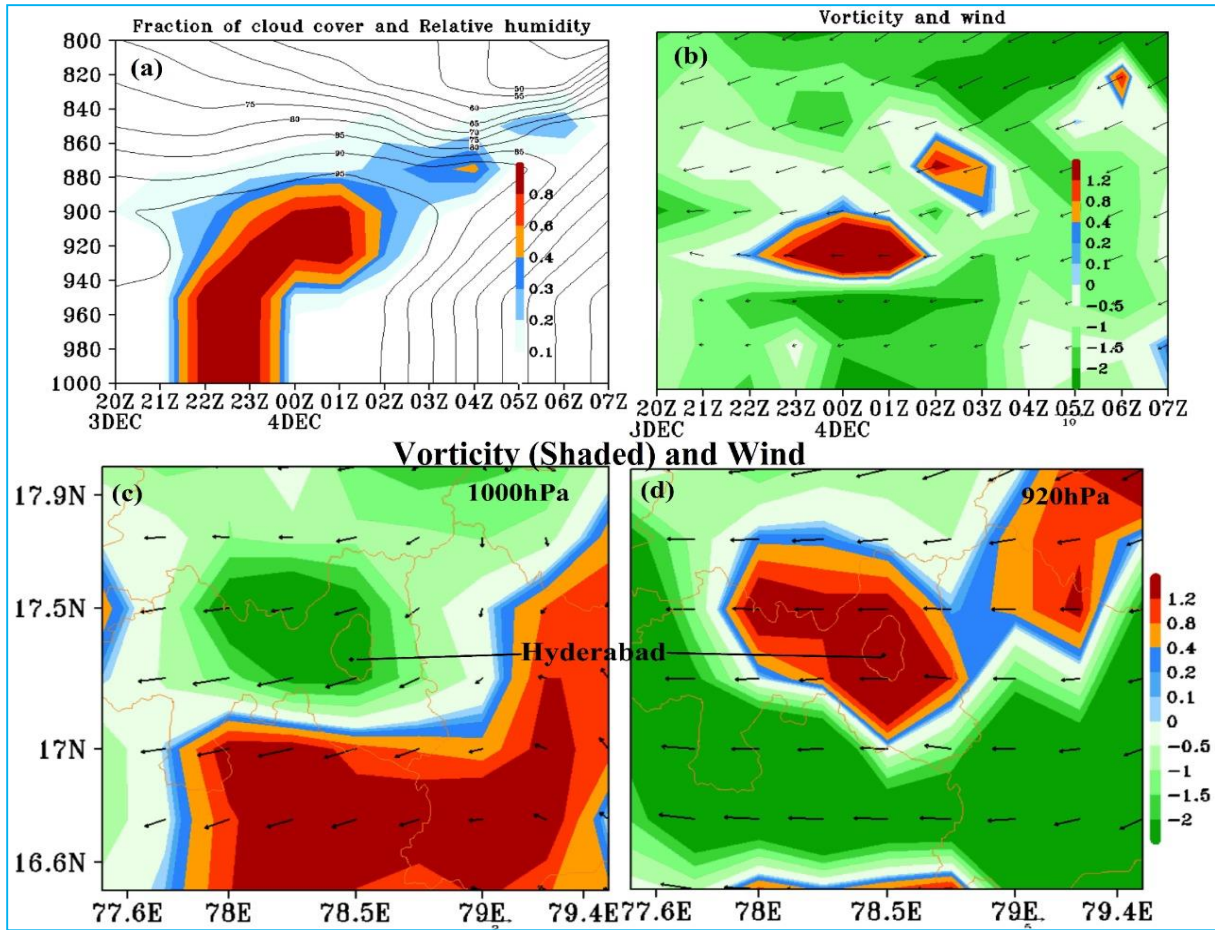
**Long event fog duration**

4 <sup>th</sup> December, 2013	
Area of event	Hyderabad
Latitude and longitude	17° 14' 5.9" N, 78° 25' 17.9" E
Onset time	0000 UTC (0530 IST) (4-hour duration)

[6<sup>th</sup> December, 2011, 0300 UTC (onset hour)] events for heights 50, 100 and 500 meters at the atmospheric boundary layer. All the cases show the transport of particles/particulates from east and northeast, indicating north-easterly and easterly winds generally prevail in December, January and February.

*3.3. Meteorological observational aspects during long-duration fog event*

During the reference period, three episodes of long-hour duration (4-hr) fog events occurred. For analysis, one such event is considered (Table 1).



**Figs. 16(a-d).** The time-height section plot of (a) fraction of cloud on the ground and relative humidity (b) vorticity and winds at various levels (c&d) vorticity and winds at 1000 hPa and 920 hPa

(i) *INSAT-3D Satellite imagery*

The INSAT-3D image [Fig. 15(a)] shows fog/low clouds indicating the prevalence of a conducive environment for long-duration fog formation. Interestingly, there are not many areas of fog except in the extreme north and central parts of the country, which indicates *in-situ* radiational fog formation.

(ii) *Meteorological parameters (METARS)*

Fog develops when the temperature difference between the air and dew point is less than 2.5 °C and is evident from the time series [Fig. 15(b)] in the early morning hours of that day. In winter months (December-February) the occurrence of fog, mist and haze late at night and early morning hours are widespread and this inference agrees with Suresh *et al.*, 2007 and Laskar *et al.*, 2013.

(iii) *Fraction of cloud cover and relative humidity*

ERA5 reanalysis for the small geographical area (16.5° N-18° N-77.5° E-79.5° E) shows widespread areal distribution of fog on the day of the event. High intense cloud cover and high relative humidity near the earth's surface persisting over the site also can be observed [Fig. 15(c)].

3.4. *Analysis of the dynamic features using reanalysis data*

The dynamical parameters that influence the formation of fog, *viz.*, cloud cover, vorticity, relative humidity, wind and vertical velocity are computed for a small geographical area (16.5° N-18° N : 77.5° E-79.5° E) covering the core of the fog region. The time-height sections of the four parameters are presented in Fig. 16. The reanalysis of ERA5 data is employed here to analyze the conditions that abet fog formation over the station.

TABLE 2

Sounding data from GPS-sonde at Hyderabad on the day of the event

Pressure (hPa)	Height (m)	Temperature (°C)	Dew Point (°C)	Relative Humidity (%)	Mixing Ratio (g/kg)	Wind Direction (Deg)	Wind speed (knot)	Lapse rate (Deg C/m)	Layer Stability
951	545	20.8	18.9	89	14.67	180	0	-	
925	770	19.0	17.7	92	13.97	100	13	0.008	
886	1142	17.8	16.5	92	13.51	90	16	0.003	
850	1498	16.4	10.4	68	9.4	80	19	0.004	
839	1609	16.3	8.8	61	8.55	80	24	0.001	
832	1681	16.2	7.8	57	8.03	80	26	0.001	
828	1722	16.2	7.2	55	7.75	78	25	0.000	Isothermal
798	2036	15.0	7.0	59	7.93	65	20	0.004	
744	2624	10.8	5.6	70	7.7	40	9	0.007	
700	3135	7.2	4.3	82	7.49	65	5	0.007	
695	3194	7.0	4.2	82	7.49	70	4	0.003	
688	3278	6.8	4.0	82	7.48	45	2	0.002	
687	3290	6.8	4.0	82	7.47	23	2	0.000	Isothermal
686	3302	6.7	3.8	82	7.39	0	1	0.008	

The time-height section of the horizontal zonal wind flow shows weakening easterlies and north-easterly flow at a lower level (from the surface upto 940 hPa) at 0000 UTC on 4<sup>th</sup> December, 2013. The corresponding downward motion field shows the diurnal variation with downward (upward) motion during the early morning. The field of horizontal divergence depicts the existence of strong divergence from the surface upto 940 hPa level from 2000 UTC on 3<sup>rd</sup> December, 2013 to 0000 UTC on 4<sup>th</sup> December, 2013. Correspondingly, regions of high humidity (90 to 99%) coincide with divergence indicating accumulation of moist air at lower levels. These dynamic features confirm the strong convection of moist air from the east and northeast flow from the coastal areas, causing the fog conditions. Additionally, the fraction of cloud (in this instance, it is a cloud on the ground) and vorticity indicate the presence of fog. The study area is blanketed by complete cloud coverage on the ground (fraction 1 indicates 100% cloud or 8 okta, 0.8 means 80% or 6 okta etc.) with copious amounts of relative humidity (RH = 100%) in and around RGIA.

Figs. 16(a-d) convey the necessary conducive conditions and confirmation of the event's occurrence. The figures explain the fraction of cloud on the ground, relative humidity, wind speed and vorticity (divergence), which are the main features of the fog event. As shown from Fig. 16(b), there are light winds and negative

vorticity and hence divergence over the studied domain up to a height of about 800 m (920 hPa). The subsidence is established from this figure. Figs. 16(c&d) depict vorticity and wind speeds at 1000 hPa and 920 hPa, respectively. It is conspicuous to note that negative vorticity (divergence) extended over Hyderabad region (vorticity below  $-2 \times 10^{-6}$  / sec) at the lower levels and positive vorticity (convergence) is visible at 920 hPa level (vorticity above  $1.2 \times 10^{-6}$  / sec) and aloft. The contiguous zone abutting the study area has positive (negative) vorticity horizontally (vertically).

The vertical extent supports the hovering of fog for a longer duration. The lighter winds support capping inversion, causing stability of the atmosphere. Stronger wind aloft indicates turbulence above 920 hPa and it limits the height of the fog.

### 3.5. Thermo-dynamic features association with fog event

The aerological diagrams provide a way to view the stable layers in the atmosphere for fog formation. The sounding data (Table 2) with negative or zero lapse rate shows inversion and isothermal layers of the atmosphere. The air aloft is observed to be interspersed with the layers that offer stable ambiance in the form of isotherms/inversions.

### 3.6. Impact on Aviation

As low visibility due to fog, mist and haze affects aviation, whether these events affected flight schedules is to be examined. The airport operations at RGIA reported that over the four years (2014-18), 17 domestic and 5 international flights were delayed due to low visibility conditions. Delays have severe economic consequences in terms of (i) disrupting later flight schedules of the same and other aircraft, (ii) incurring a loss of fuel, food to operators, (iii) opportunity and the actual cost to the passengers.

## 4. Conclusions

During the study period, mist and haze events were more frequent with longer duration, while fog events were less frequent & lasted a shorter time. Conducive meteorological factors predisposed the intensity of the duration of the events. The study infers that the considered factors offered a limited explanation for the mist and haze events. This requires further investigation. All the methods used in the study testified that climatic conditions such as humidity, calm winds, vorticity and stable layers offered a valid and reliable explanation for the formation of long-duration fog events. The vertical extent of the stable layers supports the hovering in fog for a sustaining period. The lighter winds support capping inversion, causing stability of the atmosphere. Stronger winds aloft cause turbulence, upset the stability, disperse the particulates and limit the height of the fog.

The three phenomena, fog disrupted air traffic at RGIA, Hyderabad in terms of flight delays and the consequent impact on flight schedules causing economic losses to the operators and consumers.

### Acknowledgement

The authors express their sincere gratitude to the DG, IMD, for his encouragement. The authors acknowledge the utilization of data resources from the AMO, AAI and the GMR group at RGIA. The authors also acknowledge their indebtedness to NCEP/NCAR,

NOAA ARL to make the researchers' resources and software tools available.

*Disclaimer* : The contents and views expressed in this study are the views of the authors and do not necessarily reflect the views of the organizations they belong to.

### References

- Kulkarni, Rachana, Jenamani, Rajendra, K., Pithani, P., Konwar, M., Nigam, N. and Ghude, S. D., 2019, "Loss to Aviation Economy Due to Winter Fog in New Delhi during the Winter of 2011-2016", *Atmosphere*, **10**, 4, 198. <https://doi.org/10.3390/atmos10040198>.
- Kutty, S., Agnihotri, G., Dimri, A. P. and Gultepe, I., 2019, "Fog Occurrence and Associated Meteorological Factors Over Kempegowda International Airport, India", *Pure and Applied Geophysics*, **176**, 3. doi : 10.1007/s00024-018-1882-1.
- Laskar, S. I., Bhowmik, S. K. Roy and Sinha, Vivek, 2013, "Some statistical characteristics of occurrence of fog over Patna airport", *MAUSAM*, **64**, 2, 345-350.
- Peng, Huaqing, Liu Duanyang, Zhou Bin, Su Yan, Wu Jiamei, Shen Hao, Wei Jiansu and Cao Lu., 2016, "Boundary-Layer Characteristics of Persistent Regional Haze Events and Heavy Haze Days in Eastern China", *Advances in Meteorology*, Article ID 6950154, 23 pages. <http://dx.doi.org/10.1155/2016/6950154>.
- Ram, S. and Mohapatra, M., 2008, "Some characteristics of fog over Guwahati airport", *MAUSAM*, **59**, 2, 159-166.
- Shukla, A. and Agnihotri, G., 2021, "Analysis of Fog And Inversion Characteristics Over Sub-Urban Bangalore", *MAUSAM*, **72**, 387-398.
- Suresh, R., Janakiramayya, M. V. and Sukumar, E. R., 2007, "An account of fog over Chennai", *MAUSAM*, **58**, 4, 501-512.
- Tyagi, S., Tiwari, S., Mishra, A., Singh, S., Hopke, Philip K., Singh, Surender and Attri, S. D., 2017, "Characteristics Of Absorbing Aerosols During Winter Foggy Period Over The National Capital Region of Delhi : Impact Of Planetary Boundary Layer Dynamics And Solar Radiation Flux", *Atmospheric Research*, **188**, 1-10. <https://doi.org/10.1016/j.atmosres.2017.01.001>.
- Wang, Xinfeng and Chen, Jianmin, 2014, "Fog Formation in Cold Season in Ji'nan", China : Case Analyses with Application of HYSPLIT Model, *Advances in Meteorology*, Volume **2014**, Article ID 940956, 8 pages, <http://dx.doi.org/10.1155/2014/940956>.

